CORA Cork Open Research Archive
Cartlann Taighde Oscailte Chorcaí

Title	Interesting evidence for template-induced ferroelectric behavior in ultra-thin titanium dioxide films grown on (110) neodymium gallium oxide substrates
Authors	Deepak, Nitin;Caro, Miguel A.;Keeney, Lynette;Pemble, Martyn E.;Whatmore, Roger W.
Publication date	2014-01-10
Original Citation	Deepak, N., Caro, M. A., Keeney, L., Pemble, M. E. and Whatmore, R. W. (2014) 'Interesting Evidence for Template-Induced Ferroelectric Behavior in Ultra-Thin Titanium Dioxide Films Grown on (110) Neodymium Gallium Oxide Substrates', Advanced Functional Materials, 24(19), pp. 2844-2851. doi: 10.1002/adfm.201302946
Type of publication	Article (peer-reviewed)
Link to publisher's version	https://onlinelibrary.wiley.com/doi/abs/10.1002/adfm.201302946 - 10.1002/adfm.201302946
Rights	© 2014 WILEY-VCH Verlag GmbH & Co. KGaA, Weinheim. This is the peer reviewed version of the following article: Deepak et al (2014), Interesting Evidence for Template#Induced Ferroelectric Behavior in Ultra#Thin Titanium Dioxide Films Grown on (110) Neodymium Gallium Oxide Substrates. Adv. Funct. Mater., 24: 2844-2851, which has been published in final form at https://doi.org/10.1002/adfm.201302946. This article may be used for non-commercial purposes in accordance with Wiley Terms and Conditions for Self-Archiving
Download date	2026-10-31 12:30:02
Item downloaded from	https://hdl.handle.net/10468/7725



University College Cork, Ireland
Coláiste na hOllscoile Corcaigh

Submitted to ADVANCED FUNCTIONAL MATERIALS

DOI: 10.1002/adfm.((please add manuscript number))

Article type: (Full Paper)

Title: Interesting Evidence for Template-Induced Ferroelectric Behavior in Ultra-Thin Titanium Dioxide Films Grown on (110) Neodymium Gallium Oxide Substrates

Author(s), and Corresponding Author(s) Nitin Deepak[1,2,*], Dr. Miguel A. Caro[1,3],Dr. Lynette Keeney[1],Prof. Martyn E. Pemble[1,2] and Prof. Roger W. Whatmore[1,2,4*]*

[1]Tyndall National Institute, University College Cork, 'Lee Maltings', Dyke Parade, Cork, Ireland.

[2]Department of Chemistry, University College Cork, Dyke Parade, Cork, Ireland.

[3]Department of Physics, University College Cork, Dyke Parade, Cork, Ireland.

[4]Department of Materials, Imperial College London, South Kensington Campus, London SW7 2AZ, UK

Email: nitin.deepak@tyndall.ie, roger.whatmore@tyndall.ie

Keywords: (Ferroelectrics, Strain, Chemical Vapour Deposition (CVD), Atomic Vapour Deposition (AVD), anatase, TiO_2)

Abstract

This paper reports the first-ever presentation of evidence for room-temperature ferroelectric behavior in anatase-phase titanium dioxide (a-TiO_2). It is shown that behaviour strongly indicative of ferroelectric behavior is induced in ultra-thin (20nm to 80nm) biaxially-strained epitaxial films of a-TiO_2 deposited by liquid injection chemical vapour deposition onto (110)

neodymium gallium oxide (NGO) substrates. The structural properties of the films were analyzed by x-ray diffraction and high-resolution transmission electron microscopy, which showed significant orthorhombic strain in films. Possible ferroelectric behavior was probed by piezoresponse force microscopy (PFM). The films on NGO showed a switchable dielectric spontaneous polarization, the ability to retain polarization information written into the film using the PFM tip for extended periods (several hours) and at elevated temperatures (up to 100°C) without significant loss, and the disappearance of the polarization at a temperature between 180 and 200°C, indicative of a Curie temperature within this range. This combination of effects is believed to constitute strong experimental evidence for ferroelectric behavior, which has not hitherto been reported in a-TiO_2 and opens up the possibility for a range of new devices and materials applications. A model is presented for the effects of large in-plane strains on the crystal structure of anatase which provides a possible explanation for the experimental observations.

1. Introduction

Simple transition metal oxides are widely used in modern electronic devices because they show a wide range of useful properties, such as high permittivities (e.g. HfO_x[1] used in transistor gate stacks) and switchable resistivities (e.g. TiO_2 used in memristor[2] memories). The deliberate breaking of various kinds of symmetries can induce new, interesting and applicable properties which would otherwise be absent. Examples include ferromagnetic[3] behavior in $TbMnO_3$ thin films due to breaking of time-reversal symmetry and ferroelectric[4] behavior in $SrTiO_3$ (STO) thin films due to strain-induced inversion symmetry breaking. These induced-properties promise applications in fields such as spintronics[5] and non-volatile data storage.[6] Strain-related effects have been well-studied in the recent past, especially for thin film systems,[7] where large strains can be induced by lattice mismatch between the film and the substrate. Enhancements in T_c (critical temperature) were observed in ferroelectric,[8]

ferromagnetic[9] and even superconducting materials.[10] Properties such as induced ferromagnetism and superconductivity have been observed due to broken symmetries at the interface[11] between a $LaAlO_3$ substrate and a $SrTiO_3$ film. Recently, strain-induced ferroelectric behavior has been observed in ca 10nm thick films of HfO_2[12] and $Zr_{0.5}Hf_{0.5}O_2$[13] on silicon. The appearance of ferroelectricity in oxide thin films with such simple compositions, when compared with conventional oxide ferroelectrics such as $PbZr_xTi_{1-x}O_3$ is particularly interesting, as it offers the possibility for much easier integration of materials with useful active properties such as piezoelectricity, pyroelectricity, switchable polarization etc. with active semiconductor devices on silicon and III-V compounds. These discoveries have been facilitated by the use of advanced growth techniques such as molecular-beam epitaxy (MBE) ,[14] pulsed laser deposition (PLD) ,[15] chemical vapour deposition (CVD)[16] and atomic layer deposition (ALD)[17] that have made-possible the deposition of single crystalline thin films with atomic level precision.

TiO_2 is a cheap, extremely versatile material that exists in four crystalline forms in the bulk, including anatase & rutile (both tetragonal, 4/mmm), brookite (orthorhombic,2/mmm) and akaogiite[2] (monoclinic, 2/m). All of these forms of TiO_2 are centrosymmetric and therefore are both non-piezoelectric and non-ferroelectric. Grünebohm *et al*.[18] performed first-principle calculations on rutile-phase TiO_2 , which indicated the possibility of phonon mode softening under (110) strain and strain-induced ferroelectricity, but to date, there has been no experimental confirmation of ferroelectric behavior in rutile or any of the other TiO_2 crystalline phases. Here, we report the first experimental observations of possible ferroelectric behavior in thin anatase titanium dioxide (a-TiO_2) films grown on (110) $NdGaO_3$ (NGO) substrates, providing clear experimental evidence for the still-further expansion of the versatility of this material.

2. Results and Discussion

Highly *c*-axis oriented a-TiO_2 thin films were grown by liquid injection chemical vapour deposition (LI-CVD), sometimes referred to as atomic vapour deposition (AVD) onto 0.5mm-thick (110) NGO and (001) STO substrates. (These will be referred to hereafter as a-TiO_2/NGO and a-TiO_2/STO films). All growth details are provided in the experimental section. Bragg-Brentano XRD scans confirmed that the a-TiO_2/NGO and a-TiO_2/STO films are single phase anatase (**Figure S3**) with thicknesses ranging from 20 nm to 100 nm. XRD phi scans of the asymmetrical (101) anatase peak for 20 nm films showed only four peaks, confirming that the films were grown epitaxially on both substrates (Figure S4). The epitaxial relationships between film and substrate are (001)[100] a-TiO_2 || (110)[1-10] NGO & (001)[010] a-TiO_2 || (110)[001] NGO and (001)[100] a-TiO_2 || (001)[100] STO & (001)[010] a-TiO_2 ||(001)[010] STO. Cross-sectional TEM (Figure S5) showed excellent crystalline quality with a sharp film/substrate interface.

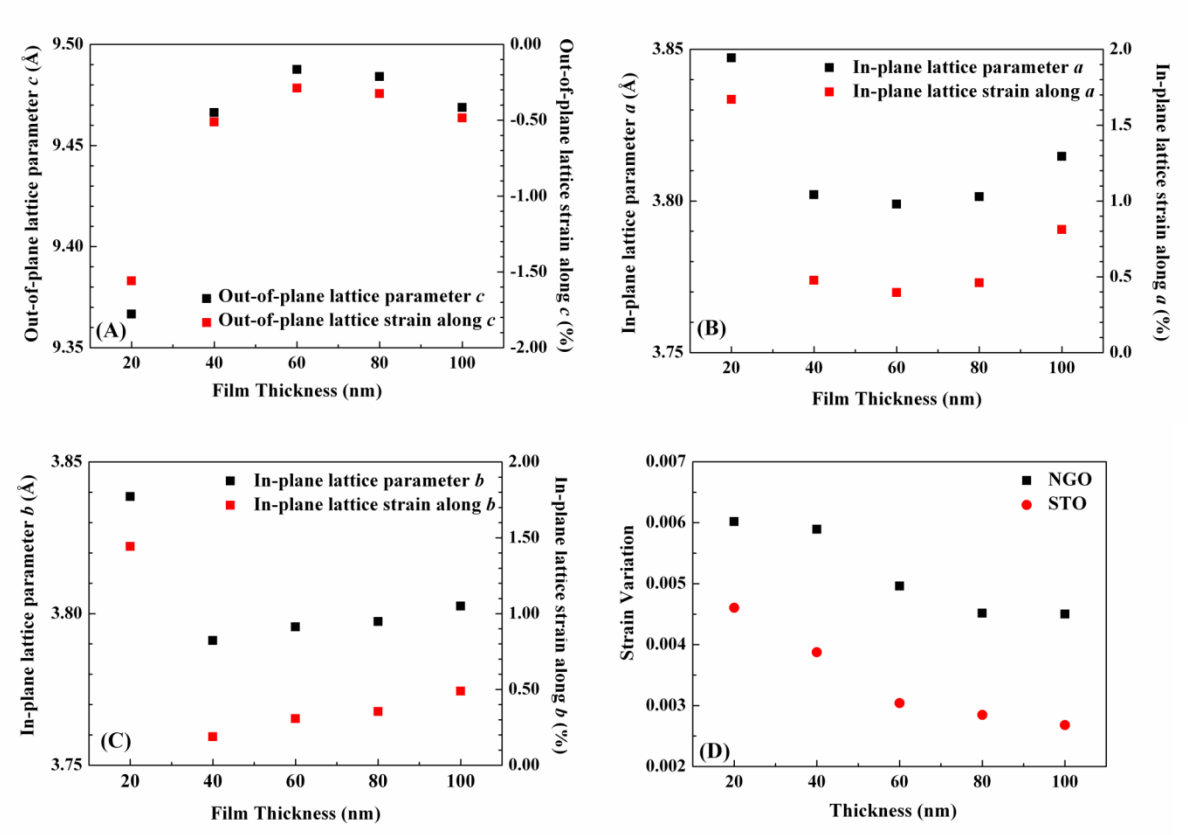


Figure 1. The change in lattice parameter and strain **(A)** out-of-plane *c* **(B)** in-plane *a* **(C)** in-plane *b*, with thicknesses varying from 20 nm to 100 nm for the a-TiO_2 films grown on NGO substrates and **(D)** strain

variation (estimated from peak broadening) for the a-TiO_2 films grown on NGO and STO substrates. The strain variation for 20 and 40 nm films is similar, whereas the strain variation is decreased for 60 and 80 nm films and is lowest for the 100 nm a-TiO_2 films grown on NGO substrates. All the a-TiO_2 films grown on STO, shows a monotonic deviation of strain variation with thickness.

Figure 1A shows the variation of out-of-plane lattice constants (*c*) and lattice strains for varying thicknesses of the a-TiO_2/NGO films. The *c*-axis length for bulk anatase is 9.515Å (Space group $I4_1/amd$).[19] On comparing the average value of *'c'* for the a-TiO_2/NGO films with thickness from 20nm to 100nm, it can be observed that its value changes from 9.367Å to 9.487Å for 20nm to 60nm films. However the value of *'c'* decreases at 80nm to 9.484Å and is decreased further for 100nm to 9.469Å, as compared to the 60nm thick films. The a-TiO_2/STO films showed a regular increase in the value of *c* from 9.422Å to 9.474Å on increasing film thickness from 20nm to 100nm (Figure S6). No anomaly was observed at higher thicknesses, as evident for the a-TiO_2/NGO films. The thinnest (20nm) a-TiO_2/NGO and a-TiO_2/STO films have a negative average *c*-axis strain of 1.57% and 0.97% respectively, corresponding to a substantial amount of tensile stress in the films, which decreases to ca 0.4% for the 100nm films on both substrates.

Strain is induced in the films due to lattice mismatch between the film and substrate. Recent work by Catalan et al.[20] has shown that, as for semiconducting materials, epitaxial oxides demonstrate strain relaxation with increasing thickness. The strain relaxation occurs by formation of misfit dislocations and these dislocations distribute the strain field, which causes a strain gradient. Similar to polycrystalline thin films, XRD peak broadening also gives a measure of strain variation for the epitaxial thin films.[20] If we assume that there is no variation in the composition of the film (as there are no dopants), then this peak broadening gives a direct measure of variation in *d*-spacing, or presence of a strain gradient along *c*-axis of the film, provided sample dimension (size) and instrumental broadening effects are subtracted. Specifically, the "strain broadening" is a measure of the variation of strain in the

specimen (since a uniform average strain would shift the XRD peak position). The strain broadening can be calculated by fitting the observed (004) anatase peak to a Gaussian profile and using the formula $\beta^2_{measured} = \beta^2_{strain} + \beta^2_{instrumental} + \beta^2_{size.}$ The instrumental broadening was calculated from the single crystal substrate peaks of STO and NGO. The size broadening (determined by film thickness for (00*l*) peaks), is calculated by structure factor modeling for anatase films with thicknesses from 20 nm to 100 nm (see supplementary information). The squares of instrumental and size broadening were subtracted from the experimental FWHM to obtain the broadening due to strain variation. The formula $\Delta\varepsilon = \beta_{strain}/4tan\theta$ is used to calculate the average strain variation, $\Delta\varepsilon$.[20] An interesting trend was observed for $\Delta\varepsilon$ *vs.* thickness as shown in Figure 1D for both the a-TiO_2/NGO and a-TiO_2/STO films. The 20 nm and 40 nm a-TiO_2/NGO films possess almost the same $\Delta\varepsilon$ (approx. 0.006). $\Delta\varepsilon$ decreases to 0.005 for 60 nm thickness, and becomes almost constant at 0.0045 for 80 nm and 100nm films. For the a-TiO_2/STO films there is a gradual relaxation of $\Delta\varepsilon$ from 0.0046 to 0.0027 for thicknesses from 20 to 100 nm.

The crystal structure of the NGO substrate is orthorhombic with lattice parameters[21] a = 5.4333 Å, b = 5.5036 Å, and c = 7.7157 Å. (110) oriented NGO substrates thus present in-plane lattice parameters of a' = 3.8669 Å and b' = 3.8579Å for the a-TiO_2 film growth. The in-plane lattice parameters for anatase are $a = b$ = 3.7842 Å.[19] The lattice mismatch between the NGO substrate and anatase is slightly different along the a and b directions, with values of 2.14% and 1.91% respectively. These values are slightly greater than the measured average a and b strains of 1.67 and 1.44% respectively for the thinnest 20nm films (see Figure 1), as would be expected, and confirm that an in-plane biaxial strain originates due to lattice mismatch between the film and the NGO substrate. This is supported by the variation in (101) phi-scan peak intensity, with alternate peaks being reduced in intensity due to slight differences in the in-plane lattice parameters. STO is cubic with a lattice constant a = 3.905 Å.

Thus the isotropic in-plane lattice mismatch between the a-TiO_2 thin film and STO substrate is significantly greater than for NGO at 3.098%. However, the a-TiO_2/STO films are more relaxed than the a-TiO_2/NGO films, most likely because of the increased mismatch. 20 nm a-TiO_2/NGO films possess 1.67 and 1.44% *a* and *b*-axis strains respectively, compared with 0.47% a/b axis strain for a-TiO_2/STO films. The critical thickness of the film at which the dislocation and other defects start to occur in the film will thus be smaller for films grown on STO as the critical thickness is inversely proportional to lattice mismatch.[22] Due to higher lattice mismatches, a-TiO_2 films grown on STO substrates relax more easily through defect formation when compared with films grown on NGO substrates.

Four point probe tests confirmed that the films were electrically insulating. Piezoresponse-Force Microscopy (PFM) imaging was performed on 20nm to 100 nma-TiO_2/NGO films thicknesses with 5.5V AC applied to the PFM tip (Figure 2). All films exhibited a piezoelectric response in the as-grown state. The 20nm and 40nm films show no amplitude and phase contrast, but the 60nm films show a bi-domain structure with clear 180° phase variation between adjacent domains. The absence of spatial phase and amplitude contrast for the 20nm and 40nm films is likely to be due to the high strain conditions stabilizing a single domain state, as compared to the 60nm films, where strain relaxation allows the film to form a bi-domain state.

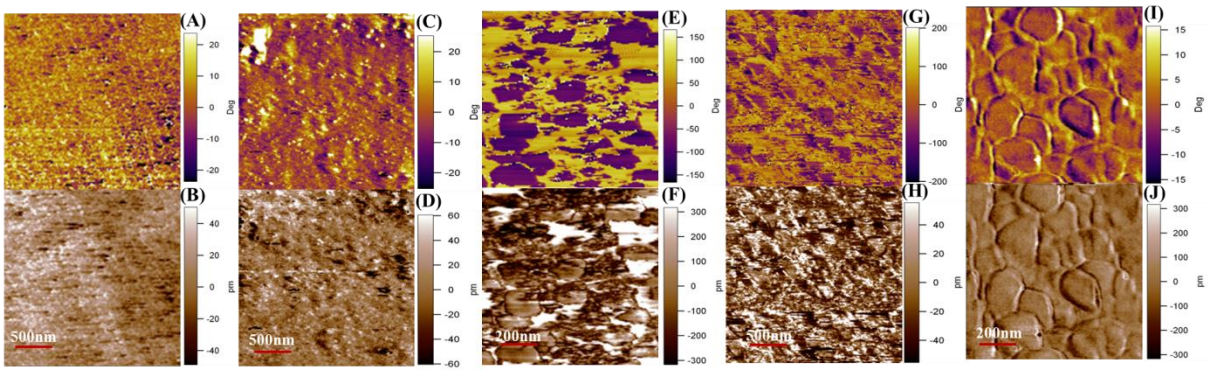


Figure 2 The variation in domain structure of a-TiO_2 thin films grown on NGO substrates. Phase and amplitude images, respectively are displayed for **(A), (B)** 20 nm, **(C), (D)** 40 nm, **(E), (F)** 60 nm, **(G)**, **(H)** 80 nm and **(I)**,

(J) 100 nm films. The 20 nm and 40 nm thin films demonstrate no phase and amplitude contrast (pointing towards a single domain structure). However, the 60 nm film shows clear 180 degree switching between yellow and purple regions and clear amplitude contrast. The scale bar is different for some images due to different feature sizes.

PFM hysteresis loop measurements were performed on 20nm to 100nm a-TiO_2/NGO films using the DART-PFM mode. Strain and phase hysteresis loops (Figure S8), were observed for films with thicknesses of 20nm to 80nm, but no hysteresis loops were observed for 100nm films. This 180° phase switching is a signature of ferroelectric behavior. Poling experiments were performed using PFM on 20nm a-TiO_2/NGO films. Five square domain patterns of size 3µm x 3µm were written by applying ± 30V DC bias to a conducting PFM tip in contact with the sample surface. PFM imaging was subsequently performed with a 5.5V AC drive signal. Figs. 3A and 3B show the PFM amplitude images immediately after poling with + 30V and -30V DC respectively.

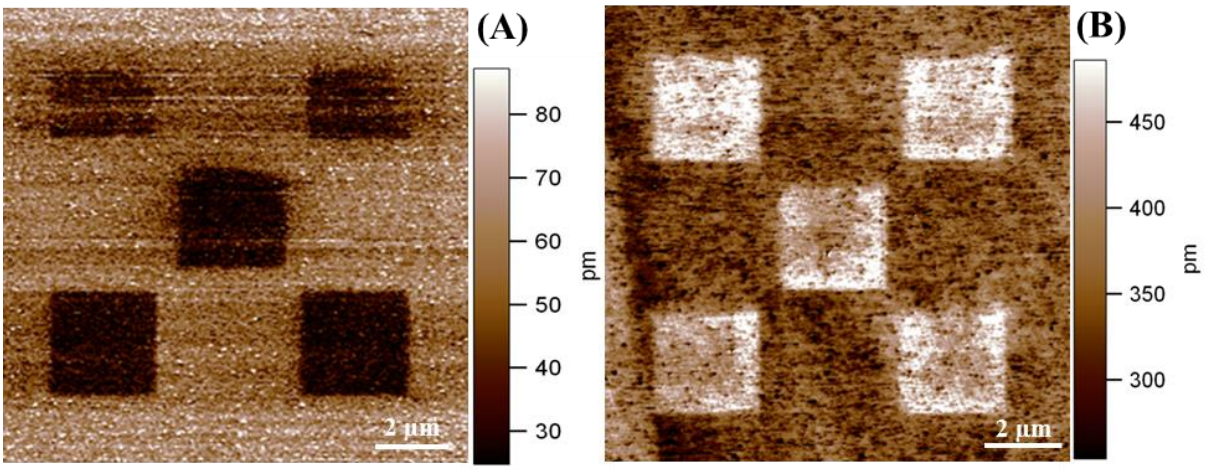


Figure 3 PFM amplitude image after poling regions of the 20 nm a-TiO_2 film grown on NGO substrate with **(A)** +30 V and **(B)** -30 V DC bias to write five 3µm x 3µm square domains. This bipolar switching confirms the stability of two polarization states.

Amplitude contrast can be clearly observed in this image. The poled domains were stable for more than 48 hours at room temperature after poling. Poling with both positive and negative bias confirms the bi-stable states and the stability of the written domain patterns over this

extended period of time points towards genuine ferroelectric behavior in a-TiO_2 thin films, rather than an effect due to charge migration (e.g. oxygen vacancy) effects. The same kinds of PFM poling experiments were performed on 20nm a-TiO_2/STO films. No amplitude contrast was observed in PFM amplitude images after poling with ±30V bias (Figure S9B). These experiments clearly show the effect of substrate on the behavior of the a-TiO_2 thin films, whereas the films grown on NGO substrates exhibit ferroelectric behavior and those grown on STO do not. Poling experiments on bare NGO substrates were performed to test the possibility of piezoresponse from the substrate or the presence of electrostatic effects. No amplitude contrast was observed from the regions of the NGO substrates subjected to the positive or negative potentials (Figure S9C). However, some contrast (shown as black in the amplitude image) was observed at the interfaces between the regions subjected to positive and negative voltages. This can be interpreted as being due to the migration of electrical charge within NGO under the applied potentials, to produce local positively and negatively charged regions. The interface between these regions would be electrically dipolar and thus be expected to give a PFM response. PFM hysteresis loop measurements were also performed on NGO substrates with voltages up to 220V DC and no hysteresis loops were observed. The fact that no hysteresis loops were observed on the uncoated NGO substrates confirms that the observed ferroelectric signature in the a-TiO_2/NGO films comes from the film itself, rather than the substrate. No evidence for ferroelectric behavior is observed in any of the a-TiO_2/STO films, indicating that the ferroelectric-like behavior observed in the a-TiO_2/NGO films comes from the film, rather than being due to some effect which is occurring at the film-substrate interface.

PFM signals can be observed due to electrostatic effects caused by the presence of surface charges, or effects related to oxygen vacancy migration under the presence of tip voltage, as has been observed in $LaAlO_3$/$SrTiO_3$ hetero-structures (Bark et. al[23]). In that study, the

movement of oxygen vacancies under the applied electric field induced a piezoresponse, as observed by PFM measurements. The authors observed that the piezoresponse in their samples decayed due to vacancy migration, reducing by a factor of two at room temperature, within about 15 minutes after poling. High temperature PFM measurements were performed to examine the possibility that free-charge or oxygen-vacancy related effects might be the reason for the observed piezoresponse in our a-TiO_2/NGO films. If the observed piezoresponse was due to charge effects, it should reduce to zero at elevated temperatures much more rapidly than at room temperature, since the migration of charges is a thermally activated process. A square domain pattern was written with +30V on the surface of the film at room temperature and then the temperature was increased to 80°C. Previous studies have shown that the activation energy for oxygen diffusion in TiO_2 is in the range of 1 to 2eV.[24]

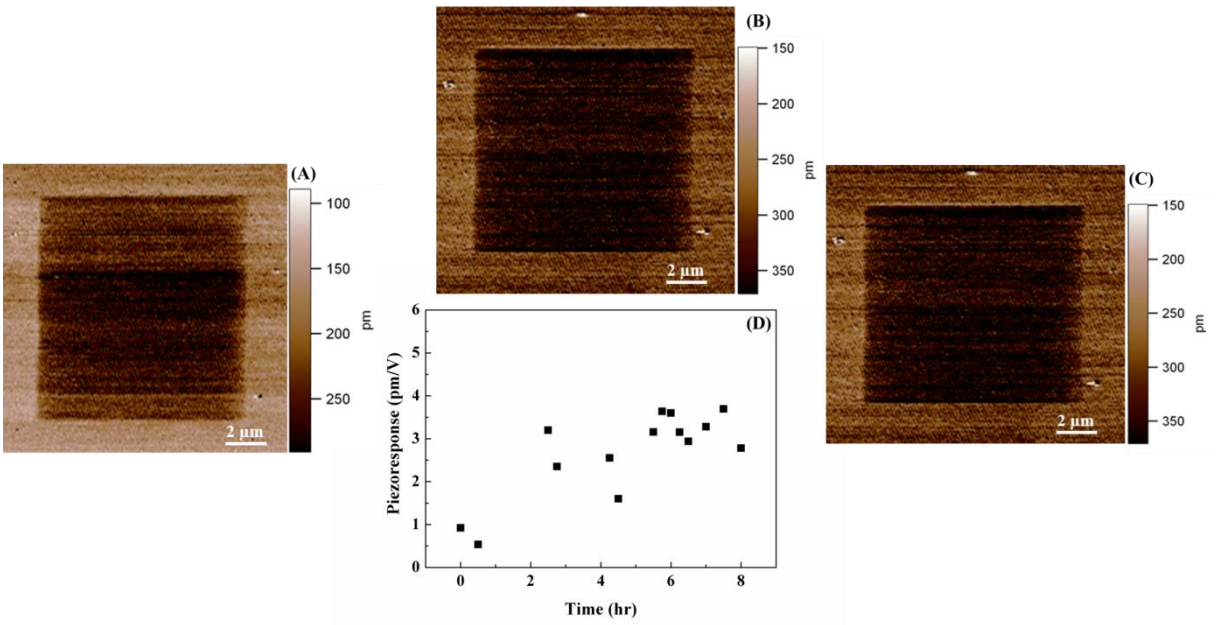


Figure 4 PFM amplitude images of a poled region (10µm x 10µm; +30V DC bias) of 20 nm a-TiO_2/NGO **(A)** 2hr, **(B)** 4hr, **(C)** 8hr of imaging at 80°C. The experiments confirm the absence of oxygen vacancy related effects and **(D)** shows the change in magnitude of the PFM amplitude over 8 hours of heating at 80°C. The piezoresponse increased significantly with time, from ~1pm/V to saturate after 3 hours at 80°C to a value of ~3.5pm/V. The increase in piezoresponse with time can be explained by the due to loss of surface moisture increasing the piezo-signal.

For 1eV activation energy, an increase in temperature from 300K to 380K would give an increase in the rate of diffusion of oxygen vacancies by a factor of about 3,000, whereas for a 2eV activation energy the rate would increase by ca10^7, a further factor of 3,000. Based on the results cited above for $LaAlO_3/SrTiO_3$ hetero-structures, we would expect the written patterns to decay away completely in a few seconds at 80°C, if they were due to oxygen vacancy migration effects. PFM imaging was performed at regular intervals over 8 hours at this elevated temperature. The written domain pattern was stable during the time of the experiment. Figures 4A,B&C show the stability of the response from the written domain at elevated temperatures as a function of time. The variation of the magnitude of the piezoresponse with time is shown in Figure 4D, which is far from decreasing, the piezoresponse actually increased significantly with time, from approximately 1 pm/V to saturate at approximately 3.5 pm/V after 3 hours of heating at 80°C. This is the reverse of what would be expected if the effect was due to charge migration and the increase is probably due to the loss of surface-bound moisture from the sample at elevated temperatures.

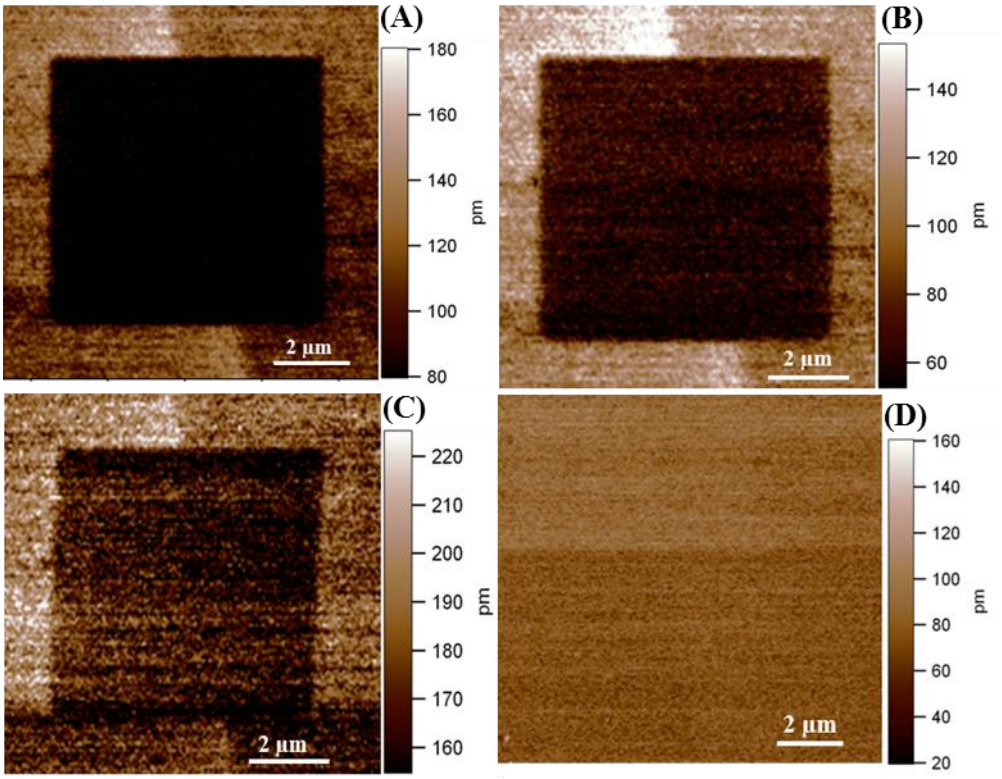


Figure 5 PFM amplitude images of a poled region (10μm x 10μm; +30V DC bias) of 20 nm a-TiO_2/NGO at **(A)** 100°C, **(B)** 150°C, **(C)** 180°C, and **(D)** 200°C. The amplitude of the poled region vanishes on heating to temperatures higher than 180°C. This observation points towards the Curie temperatures for ferroelectric a-TiO_2 lying between 180 and 200°C.

PFM experiments were also performed at higher temperatures by poling 10 μm x 10 μm region on 20nm a-TiO_2/NGO film with 30V DC bias, at room temperature and then increasing the temperatures up to 200°C. PFM imaging was performed at 100°C, 150°C, 180°C and 200°C and corresponding amplitude images are shown in Figure 5A,B,C,D respectively. The heating was performed for at least 10 minutes before imaging at each temperature.

The written domains were stable at temperatures up to 180°C. On further increasing the temperature to 200°C, the written domain vanished. The stability of the written area up to 180°C is strongly indicative that the piezoresponse is not due to charge migration, and the abrupt vanishing of the written polarization at between 180 and 200°C is a strong indication that a ferroelectric Curie temperature may lie between these two temperatures.

Piezoelectric and ferroelectric behavior only occurs in crystals whose structures lack a center of symmetry. All of the bulk crystalline forms of TiO_2 are centrosymmetric. However, Samara et al. have described rutile-phase TiO_2 as an incipient ferroelectric[25] and, as noted above, Grünebohm *et al.*[18] have discussed the theoretical possibility of ferroelectricity in rutile under certain strain conditions. Recent work on amorphous TiO_2 thin films by Kim et al[26] showed that PFM hysteresis loops and poling can be observed due to electrochemically-induced strain instead of a normal electromechanical piezoresponse. However, these films, being amorphous, could not be ferroelectric in the normal sense, and showed no domain structure. In the present case, the a-TiO_2/NGO films are fully crystalline and 60nm films show a bi-domain structure. The observation of the domain structure, the ability to switch the material bidirectionally under an applied electric field, the long-term stability of the induced polarization at elevated temperatures and the fact that the induced polarization disappears

quite sharply at a temperature between 180 and 200°C are all consistent with, and strongly indicative of, ferroelectric behavior in the a-TiO_2/NGO films. By contrast, the a-TiO_2/STO films showed none of these effects, indicating that the effects observed for the films on NGO are almost certainly not induced through an oxide-interfacial effect (such as charge trapping) at the film substrate boundary. The effect occurs only in the a-TiO_2/NGO films, for which the strain differs along the *a* and *b* axes, and both the strain magnitude and its variation within the film are much greater than that for the a-TiO_2/STO films. This is strongly indicative that the observed ferroelectric-like effects in the a-TiO_2/NGO films are strain related.

It is interesting to consider the effects that a/b strain are likely to have on the anatase crystal structure, and how these might relate to the possible occurrence of ferroelectricity. Figure 6A shows a view of the anatase crystal structure[19] at room temperature, approximately along [110]. The Ti ions sit at the centres of distorted, edge-sharing octahedra, one of which is shown in Figure 6B. There are two sets of Ti distances: O_A-Ti=1.9338Å, O_B-Ti=1.9797 Å. (The ionic radii for Ti^{4+} in 6-fold coordination by O and O are 0.605Å and 1.347Å respectively[27], so the "ideal" O-Ti distance should be 1.952Å.) The bond angle O_A-Ti-O_B is 78.1°.

The evolution of the bond lengths and bond angles in a-TiO_2 have been calculated as functions of applied in-plane strain (isotropic), from density functional theory (DFT) in the local density approximation (LDA) [28]as implemented in VASP [29] within the projector augmented wave (PAW) method .[30]

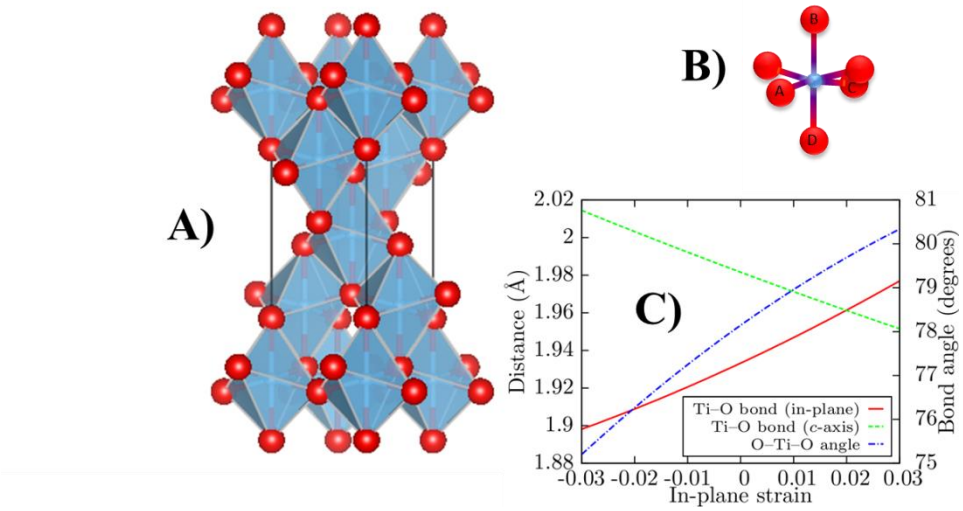


Figure 6 (A) The crystal structure of anatase (looking approximately down [110]). **(B)** One distorted TiO_6 octahedron. **(C)** The calculated (DFT-LDA approximation) change in in-plane bond length, out-of-plane bond length, and bond angle due to in-plane strain.

The energy cut-off for plane waves is 600 eV and the *k* mesh is 4x4x2 Gamma-centred. For each in-plane strain configuration, the cell dimension along the c-axis and the internal degrees of freedom of the atoms within the unit cell were allowed to relax until vanishing stress along the c-axis was obtained. The results are shown in Figure 6C and portray both the effects of cell distortion and internal strain relaxation. It is well known that LDA underestimates experimental equilibrium bond lengths. Therefore, to permit comparison of the bond lengths as a function of strain with actual values, the calculated theoretical lattice parameters (a=3.751 A and c=9.473 A) at zero in-plane strain have been normalized to the corresponding experimental values (a=3.784 A and c=9.515 A). We see that the effect of the in-plane tensile strain is to increase the in-plane Ti-O bond length and reduce the Ti-O bond length to the apical oxygens, so that at 1.7% strain they are almost equal, with O_A-Ti=1.957Å and O_B-Ti=1.964 Å. It is interesting to compare these bond lengths with the Ti-O bond lengths occurring in some perovskite compounds. In $SrTiO_3$ (STO), Ti-O=1.952 Å,[31] and for $BaTiO_3$ (BTO) Ti-O=2.05Å at T_C, and in the ferroelectric tetragonal phase at 25°C they are 1.996Å (in the a-b plane) and 2.138 & 1.898Å (along the c-axis)[32]. Hence, the calculated Ti-O bond

lengths for the 1.7% in-plane strained anatase structure sit between those for non-ferroelectric STO, which is an incipient ferroelectric and is known to become ferroelectric under strain[4], and the classic ferroelectric BTO. The Slater model of ferroelectricity[33] interprets the move from non-ferroelectric behavior in $CaTiO_3$, through incipient ferroelectricity in STO to full ferroelectric behavior in BTO as being due to the growth of the perovskite lattice as the A-cation ionic radius increases, which allows the Ti ion to move or "rattle" within the TiO_6 octahedron, increasing polarizability. Although this is an old model, there is good evidence that BTO sits at the boundary between order-disorder and soft mode behavior[34], and that the Slater model still has a good deal of utility. In the case of strongly in-plane strained anatase, it may be that the consequential distortion of the octahedra, which makes the Ti-O bond lengths much more equal so that they lie between the values occuring in STO and BTO is possibly allowing the a-TiO_2 structure to become ferroelectric. Opening the structure through in-plane tensile strain may create a situation where the Ti^{4+} can take-up a displaced position closer to one or other of the apical oxygens (O_B or O_D), to bring the Ti-O bond length on one side closer to the "ideal" value of ca 1.95Å. This would create a Ti^{4+} displacement, relative to the oxygen framework, which (because the unstrained structure is non-polar) should be switchable, leading to ferroelectricity. The relative ease of cation movement along the c-axis in anatase is supported by the high relative permittivity (38) in the un-strained material.[35] Furthermore, the fact that the effect is not seen in the films grown on STO, which exhibit a much lower level of in-plane strain, would support this model. Further more-detailed structural calculations, which will permit this model to be tested, are currently in-progress.

It is possible that a strain gradient through the films (i.e. a flexoelectric effect[36]) may also be having an effect in breaking the symmetry along the *c*-axis, and stabilising a single domain state in the thinnest films. Lee at al.[37] show that for $HoMnO_3$ thin films, a large strain gradient can stabilise the single domain structure due to the flexoelectric effect. The absence

of domains for 20 and 40 nm a-TiO_2/NGO films may be due to stabilization of single domain structure due to large strain variations and as the strain variation lessens the bi-domain structure arises for 60 nm films. Significantly more work would be needed to test this idea for the a-TiO_2/NGO films.

The fact that a-TiO_2 thin films can show strong evidence for ferroelectric behavior, if suitably strained, is a very interesting and significant observation. As noted above, previous reports on strained thin films of HfO_2 and HfO_2-ZrO_2 have also indicated ferroelectric behavior. Those films were reported to possess the monoclinic baddeleyite structure, in which the cations are 7-fold coordinated by oxygen [38] at distances between 2.05 and 2.28Å. The baddeleyite structure is very different from anatase, because the central cations are much larger than Ti^{4+} (Zr^{4+} and Hf^{4+} - 0.76 and 0.78Å respectively in 7-fold coordination by O)[27], and this is reflected in the significantly lower relative permittivities of these oxides (ca 12.5) relative to anatase. Indeed, given that ferroelectric behavior has been reported in HfO_2 and HfO_2-ZrO_2, it seems surprising that evidence for strain-induced ferroelectric behavior has never before been reported in anatase, which is a material of considerable technological-importance.

Conclusions

Single crystal thin films of anatase phase titanium dioxide of between 20 and 100 nm thick have been grown onto (001) STO and (110) NGO single crystal substrates using liquid injection chemical vapour deposition. A good epitaxial relationship has been shown in both cases, with a significantly higher level of both uniform strain and strain variation in the film in the case of NGO. PFM assessment has shown that the films on NGO exhibit a number of characteristics which strongly point to the existence of ferroelectricity in these films. These include: a bipolar domain structure, an electrically switchable polarization, which is stable with time, both at room temperature and at elevated temperatures, and the disappearance of the switched polarization (piezoelectric response) at a temperature between 180 and 200°C,

indicative of existence of a Curie temperature. It has been demonstrated that neither the a-TiO_2/STO films, nor the naked NGO or STO substrates, show these behaviors, indicating that the observed effects for the a-TiO_2 films on NGO are not substrate related, nor are they related to the existence of a film-substrate interface. We therefore conclude that the effects observed are most-likely to be due to the existence of ferroelectricity in the a-TiO_2/NGO films, which is caused by their highly-strained nature (much more highly strained than the films on STO) and the remarkable persistence of this strain throughout films of up to 100 nm. The observed high degree of strain variability through the films may be stabilising a single domain state in the thinnest films via flexoelectricity. A model is proposed here in which the in-plane tensile strain distorts the structure, making the in-plane and out of plane Ti-O bond lengths much more similar, and lying between those of STO and BTO, permitting switchable Ti *c*-axis displacements within the TiO_6 octahedra. This first observation of evidence for ferroelectricity in highly-strained anatase-phase TiO_2 thin films is remarkable, in that the distorted TiO_6 octahedra in anatase form a structural unit in which the Ti-O bond lengths might be considered to invite a bi-stable electrical displacement along the crystallographic *c*-axis, if the structure could be appropriately modified. The work reported here appears to have achieved this for the first time. Further work is now required to explore the effects in more detail, to determine the reasons for their occurrence and explore whether they are indeed due to the appearance of ferroelectricity. In particular, the deposition of highly strained epitaxial films onto pre-electroded NGO substrates would be highly desirable as it would permit the fabrication of capacitor structures to allow the study of dielectric properties, especially in the temperature range from 180 to 200°C and above. This would allow the exploration of whether the films, for example, exhibit Curie-Weiss dielectric behaviour. Other studies which may prove fruitful would include Raman spectroscopy, especially in elevated temperature

range, so see if there is any evidence for new phonon modes which may provide further evidence for ferroelectricity.

Experimental Section

a-TiO_2 thin films, with thickness ranging from 20-100nm, were deposited using a liquid injection chemical vapour deposition (atomic vapour deposition - AVD) [39] system on (110) $NdGaO_3$(NGO) and (001) $SrTiO_3$(STO) substrates. The temperature of the substrate was kept at 650°C during growth. The vaporizer was kept at 220°C. The pressure inside the growth chamber was 10 mbar. 0.1 M solution of $Ti(O\text{-}iPr)_2(thd)_2$ (where O-iPr = iso-propoxide and thd = 2,2,6,6-tetramethyl-3,5- heptanedionate) in toluene were used as a precursors. Pure oxygen and nitrogen were used as oxidizing and carrier gases respectively. The nitrogen: oxygen ratio was kept to 3:1 during the growth.

X-ray diffraction (XRD) experiments were performed with Panalytical MRD XRD system on the a-TiO_2 thin films with a filtered radiation. Transmission electron microscopy (TEM) studies were performed with a Jeol 2100 TEM on a polished sample prepared by focused ion beam (FIB) procedures on 20 nm a-TiO_2/NGO. Piezoresponse force microscope (PFM) was used in resonance enhanced Dual AC Resonance Tracking PFM (DART-PFM)[40] mode on Asylum Research MFP-3D^{TM} AFM system in contact mode at 300 ± 3Hz frequency to analyze the out-of-plane piezoelectric and ferroelectric behavior.

Supporting Information

Supporting information is provided with the attached files.

Acknowledgements

The authors acknowledge ICGEE (International Centre for Graduate Education in Micro & Nano Engineering) for funding Nitin Deepak's PhD. The support of Science Foundation Ireland (SFI) under the FORME Strategic Research Cluster Award number 07/SRC/I1172 is

greatly acknowledged. This research was also enabled by the Higher Education Authority Program for Research in Third Level Institutions (2007-2011) via the INSPIRE program.

Received: ((will be filled in by the editorial staff))

Revised: ((will be filled in by the editorial staff))

Published online: ((will be filled in by the editorial staff))

[1] K. Nomura, M. Hirano, Science 2003, 300, 1269.

[2] J. J. Yang, M. D. Pickett, X. Li, D. A. A. Ohlberg, D. R. Stewart, R. S. Williams, Nature Nanotechnology 2008, 3, 429

[3] X. Marti, V. Skumryev, C. Ferrater, M. V. García-Cuenca, M. Varela, F. Sánchez, J. Fontcuberta, Applied Physics Letters 2010, 96, 222505.

[4] J. H. Haeni, P. Irvin, W. Chang, R. Uecker, P. Reiche, Y. L. Li, S. Choudhury, W. Tian, M. E. Hawley, B. Craigo, A. K. Tagantsev, X. Q. Pan, S. K. Streiffer, L. Q. Chen, S. W. Kirchoefer, J. Levy, D. G. Schlom, Nature 2004, 430, 758.

[5] M. Bibes, A. Barthélémy, IEEE Transactions on Electron Devices 2007, 54, 1003.

[6] J. F. Scott, Nature Materials 2007, 6, 256.

[7] D. G. Schlom, L.-Q. Chen, C.-B. Eom, K. M. Rabe, S. K. Streiffer, J.-M. Triscone, Annu. Rev. Mater. Res. 2007, 37, 589.

[8] K. J. Choi, M. Biegalski, Y. L. Li, A. Sharan, J. Schubert, R. Uecker, P. Reiche, Y. B. Chen, X. Q. Pan, V. Gopalan, L.-Q. Chen, D. G. Schlom, C. B. Eom, Science 2004, 306, 1005.

[9] R. S. Beach, J. A. Borchers, A. Matheny, R. W. Erwin, M. B. Salamon, B. Everitt, K. Pettit, J. J. Rhyne, C. P. Flynn, Physical Review Letters 1993, 70, 3502.

[10] H. Sato, M. Naito, Physica C 1997, 274, 221.

[11] J. A. Bert, B. Kalisky, C. Bell, M. Kim, Y. Hikita, H. Y. Hwang, K. A. Moler, Nature Physics Letter 2011, 7, 767.

[12] T. S. Böscke, J. Müller, D. Bräuhaus, U. Schröder, U. Böttger, Applied Physics Letters 2011, 99, 102903.

[13] J. Müller, T. S. Böscke, D. Bräuhaus, U. Schröder, U. Böttger, J. Sundqvist, P. Kücher, T. Mikolajick, L. Frey, Applied Physics Letters 2011, 99, 112901.

[14] B. A. Joyce, Reports on Progress in Physics 1985, 48 1637.

[15] H. M. Christen, G. Eres, J. Phys.: Condens. Matter 2008, 20, 1.

[16] K. L. Choy, Progress in Materials Science 2003, 48, 57.

[17] M. Leskela, M. Ritala, Thin Solid Films 2002, 409, 138.

[18] A. Grünebohm, C. Ederer, P. Entel, Phys. Rev. B 2011, 84, 132105.

[19] M. Horn, C. F. Schwerdtfeger, E. P. Meagher, Zeitschrift für Kristallographie - Crystalline Materials 1972, 136, 273.

[20] G. Catalan, B. Noheda, J. McAneney, L. J. Sinnamon, J. M. Gregg, Physical Review B 2005, 72, 020102(R).

[21] T. Ohnishi, K. Takahashi, M. Nakamura, M. Kawasaki, M. Yoshimoto, H. Koinuma, Applied Physics Letters 1999, 74, 2531.

[22] A. Jasik, K. Kosiel, W. Strupifiski, M. Wesolowski, Thin Solid Films 2002 412, 50.

[23] C. W. Bark, P. Sharma, Y. Wang, S. H. Baek, S. Lee, S. Ryu, C. M. Folkman, T. R. Paudel, A. Kumar, S. V. Kalinin, A. Sokolov, E. Y. Tsymbal, M. S. Rzchowski, A. Gruverman, C. B. Eom, Nano Lett. 2012, 12, 1765−1771.

[24] J. Shi, D.-K. Lee, H.-I. Yoo, J. Janek, K.-D. Becker, Physical Chemistry Chemical Physics 2012, 14, 12930.

[25] G. A. Samara, P. S. Peercy, Phys. Rev. B 1973, 7, 1131.

[26] Y. Kim, A. N. Morozovska, A. Kumar, S. Jesse, E. A. Eliseev, F. Alibart, D. Strukov, S. V. Kalinin, ACS Nano 2012, 6, 7026.

[27] R. D. Shannon, C. T. Prewitt, Acta Crystallographica Section B 1969, 25, 925.

[28] J. P. Perdew, A. Zunger, Physical Review B 1981, 23, 5048.

[29] G. Kresse, J. Furthmuller, Phys. Rev. B 1996, 54, 11169.

[30] P. E. Blöchl, Phys. Rev. B 1994, 50, 17953; G. Kresse, D. Joubert, Phys. Rev. B 1999, 59, 1758.

[31] K. H. Hellwege, A. M. Hellwege, Vol. 16, Springer, Berlin, 1981, 59.

[32] J. Harada, T. Pedersen, Z. Barnea, Acta Crystallographica Section A 1970, 26, 336; R. Clarke, Journal of Applied Crystallography 1976, 9, 335.

[33] J. C. Slater, Physical Review 1950, 78, 748.

[34] A. Bussmann-Holder, Journal of Physics: Condensed Matter 2012, 24, 273202.

[35] B. H. Park, L. S. Li, B. J. Gibbons, J. Y. Huang, Q. X. Jia, Applied Physics Letters 2001, 79, 2797.

[36] T. D. Nguyen, S. Mao, Y.-W. Yeh, P. K. Purohit, M. C. McAlpine, Advanced Materials 2013, 25, 946.

[37] D. Lee, A. Yoon, S. Y. Jang, J.-G. Yoon, J.-S. Chung, M. Kim, J. F. Scott, T. W. Noh, Physical Review Letters 2011, 107, 057602.

[38] R. Ruh, P. W. R. Corfield, Journal of the American Ceramic Society 1970, 53, 126.

[39] P. F. Zhang, N. Deepak, L. Keeney, M. E. Pemble, R. W. Whatmore, Applied Physics Letters 2012, 101, 112903.

[40] B. J. Rodriguez, C. Callahan, S. V. Kalinin, R. Proksch, Nanotechnology 2007, 18, 475504.

Submitted to ADVANCED FUNCTIONAL MATERIALS

Supporting information

for *Adv. Funct. Mater.*, DOI: 10.1002/adfm.((please add manuscript number))

Title: Ferroelectric behavior in ultra-thin titanium dioxide films

Nitin Deepak, Lynette Keeney, Martyn E. Pemble and Roger W. Whatmore**

To whom correspondence should be addressed: nitin.deepak@tyndall.ie or roger.whatmore@tyndall.ie

This file includes:

1. Size broadening calculations for (004) XRD Anatase peak

2. Figures S1 to S11

Size broadening calculations for (004) XRD Anatase peak

The a-TiO_2 films grown on NGO and STO are highly *c*-axis oriented and epitaxial, as can be observed from XRD data shown in Figure S3 and S4 respectively. In order to calculate the size broadening effects for highly oriented a-TiO_2 thin films, the structure factor can be calculated along the *c*-direction for various number of TiO_2 layers. The structure factor is calculated for '$\boldsymbol{n}$' number of layers of TiO_2 with lamella of length '$\boldsymbol{L}$' such that the thickness $\boldsymbol{h = nc}$, where $\boldsymbol{c}$ is the out-of-plane lattice parameter for anatase as shown in Figure S1.
The equation used for calculating the structure factor F(s) for rectangle ABCD is

$$\mathbf{F(s) = \phi\,(s)}\sum_{j=1}^{n}\left[\boldsymbol{L}\exp\left(i2\Pi s x_j\right)\right] \quad \text{(S1)}$$

where $\boldsymbol{\varphi\,(s)}$ is the scattering factor for one unit cell of a-TiO_2 , $\boldsymbol{s = 2sin\theta/\lambda}$ and $\boldsymbol{x_j}$ is 0 , c , 2c, ….., nc for j = 1, 2, 3 ….., nc respectively. The $\boldsymbol{\varphi\,(s)}$ is calculated using following equation

$$\boldsymbol{\phi\,(s)} = \sum_{j=1}^{m}\left[f_i\exp\left(i2\Pi s y_j c\right)\right] \quad \text{(S2)}$$

where $\boldsymbol{f_i}$ is the scattering factor for different values of $\boldsymbol{s}$ for individual $\mathbf{Ti^{4+}}$ atoms with $\boldsymbol{y_i}$ as their fractional co-ordinates along *c*-axis in anatase unit cell. The value of **L** is kept constant to 1µm.
The value of $\boldsymbol{n}$ is changed to calculate the broadening due to size for the (004) anatase peak for approximate thicknesses of 20, 40, 60, 80 and 100 nm respectively. The effect of thickness on the FWHM (full width half maximum) can be calculated without including any other factor (such as instrumental and strain effects) and is shown in Figure S2.

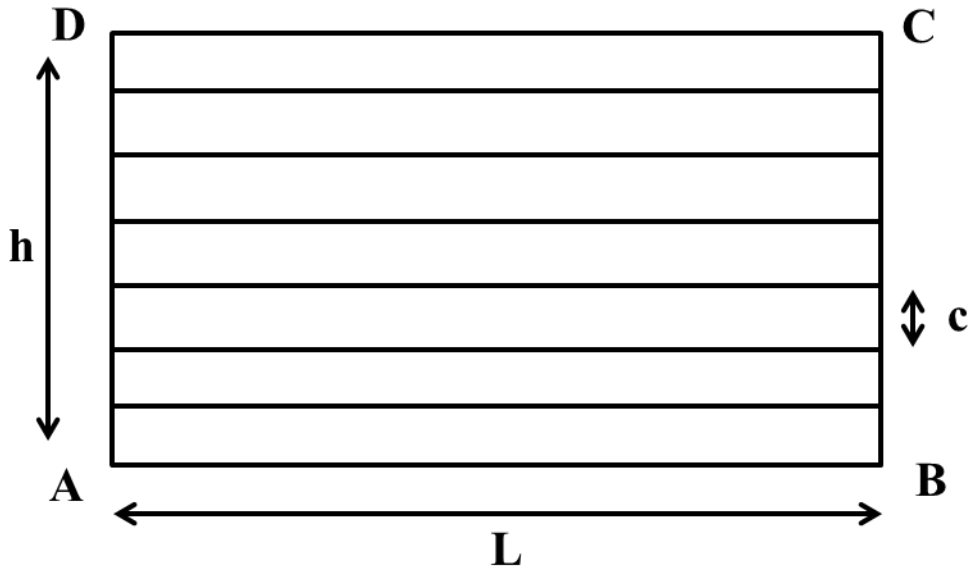


Figure S1 The rectangle ABCD with length **L** and height **h** with distance between each plane **c** used to calculate the size broadening effect for a-TiO_2 structure.

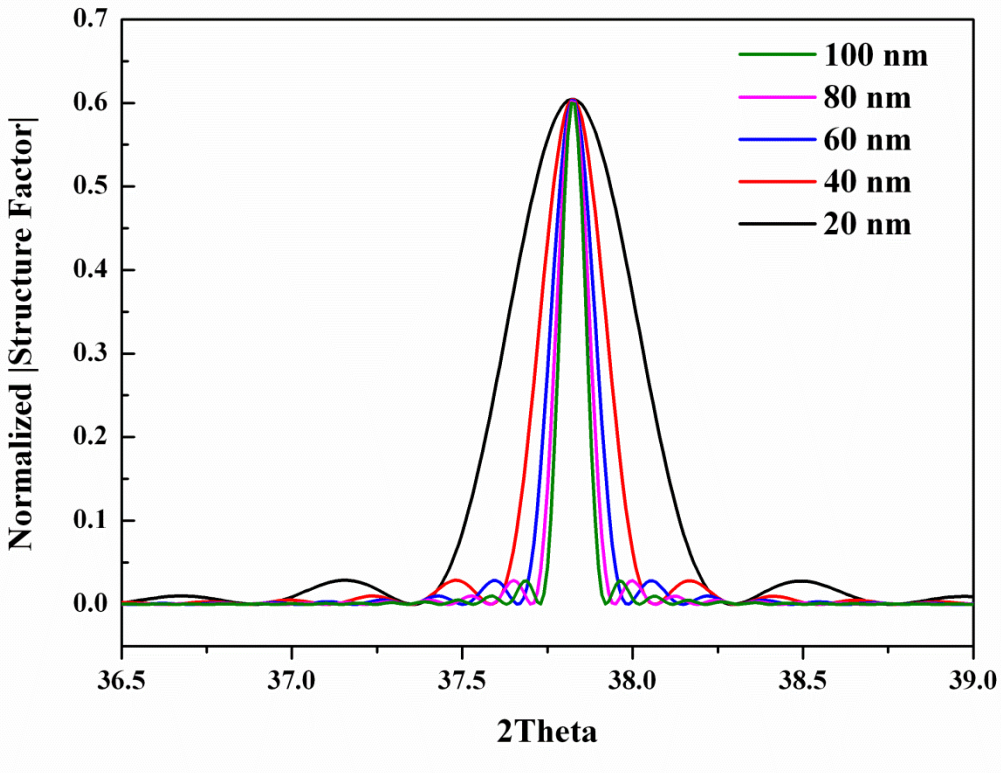


Figure S2 The effect of thickness on the FWHM of (004) anatase peak.

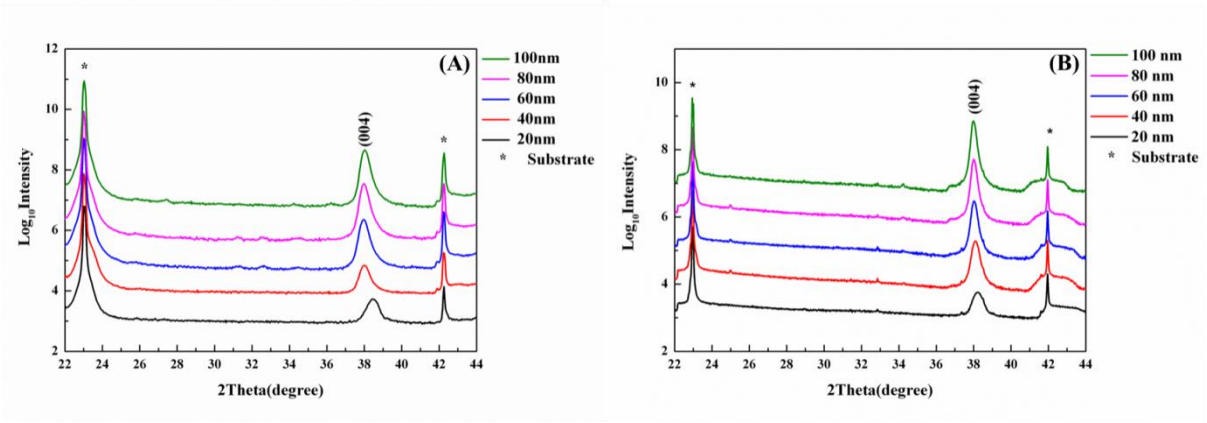


Figure S3 Theta-2Theta XRD scans for a-TiO_2 films grown on **(A)** NGO substrates and **(B)** STO substrates for thicknesses 20 nm to 100 nm. The films are highly *c*-axis oriented. The only detectable phase in the films with XRD was anatase.

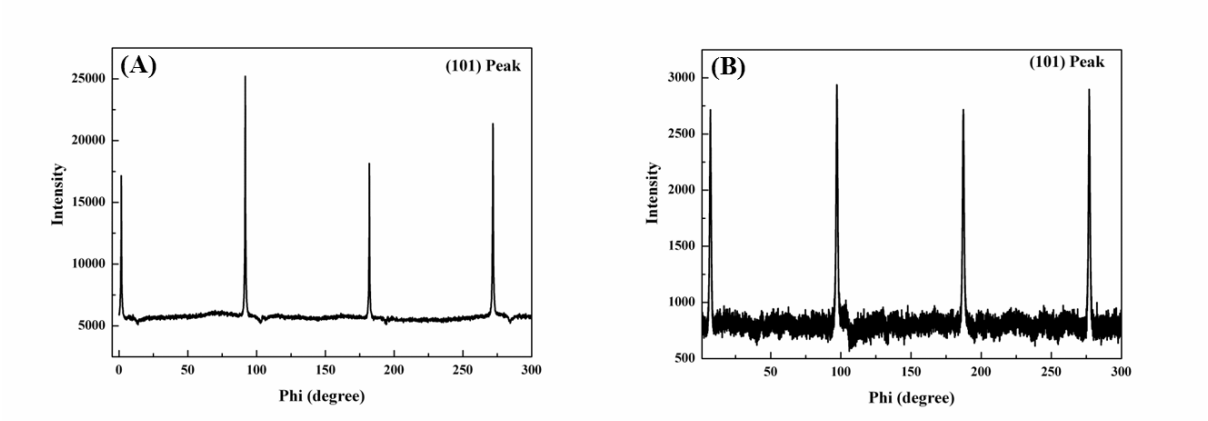


Figure S4 XRD phi-scan of asymmetrical (101) peak confirming the epitaxial nature for 20nm a-TiO_2 film grown on **(A)** NGO and **(B)** STO substrates.

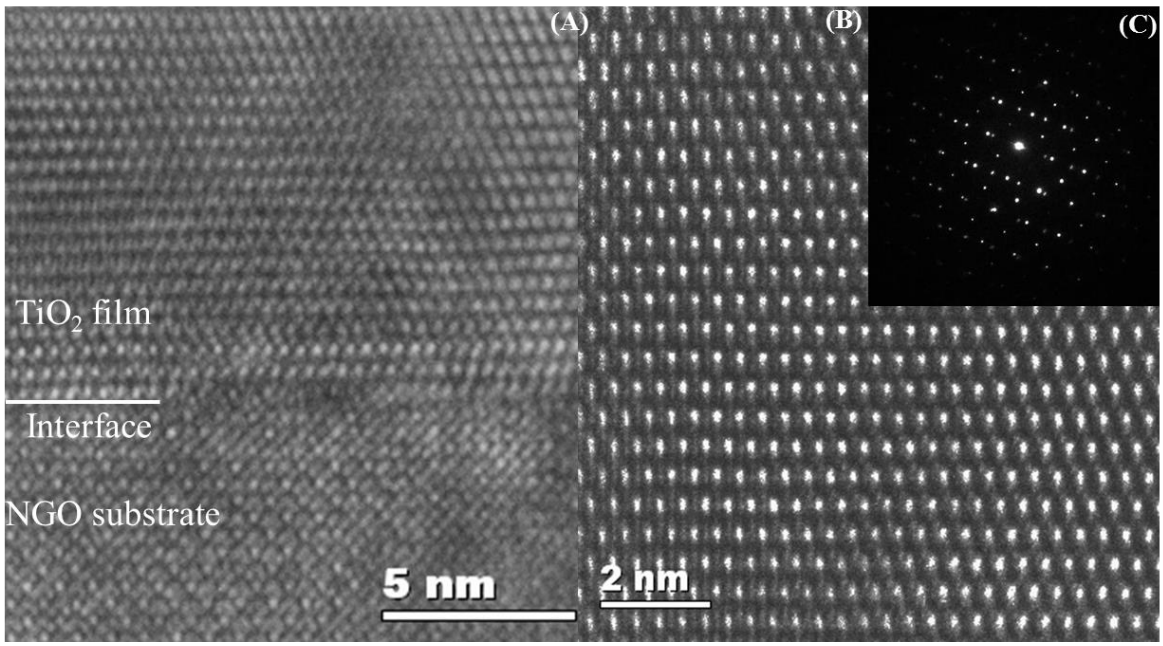


Figure S5 TEM images of 20 nm **(A)** a-TiO_2 film and substrate interface, **(B)** a-TiO_2 film and **(C)** selected area diffraction pattern (SAED) for film + substrate grown on NGO substrate.

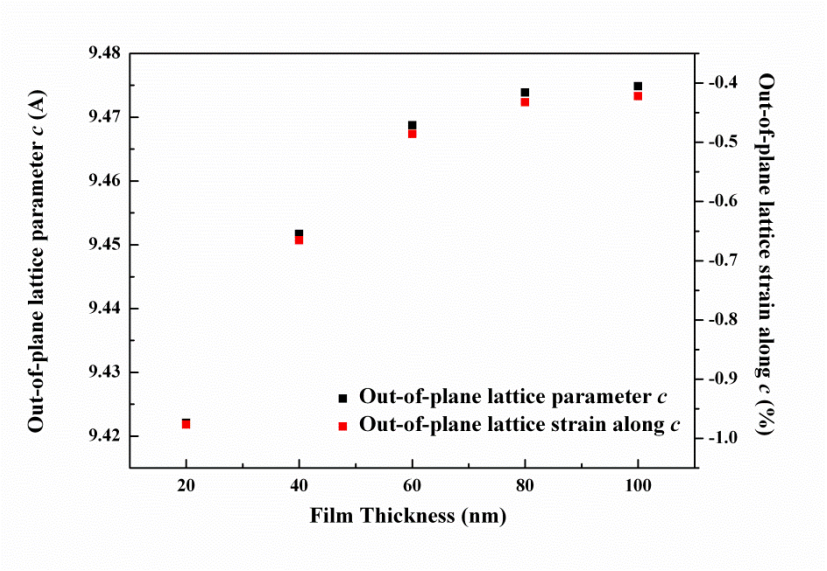


Figure S6 The effect of thickness on out-of-plane lattice parameter (*c*) and out-of-plane lattice strain for the a-TiO_2 films grown on STO substrates.

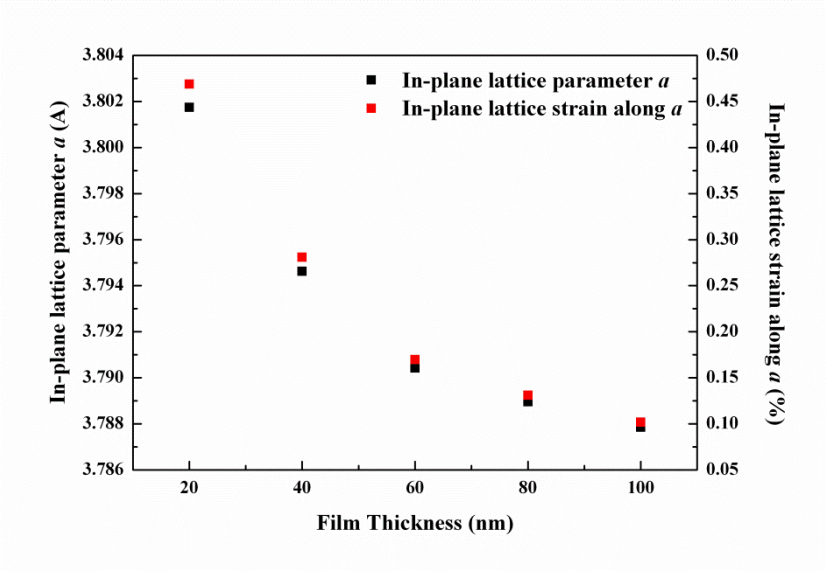


Figure S7 The effect of thickness on in-plane lattice parameter and in-plane lattice strain along **a** *a*-direction for the films grown on STO substrates.

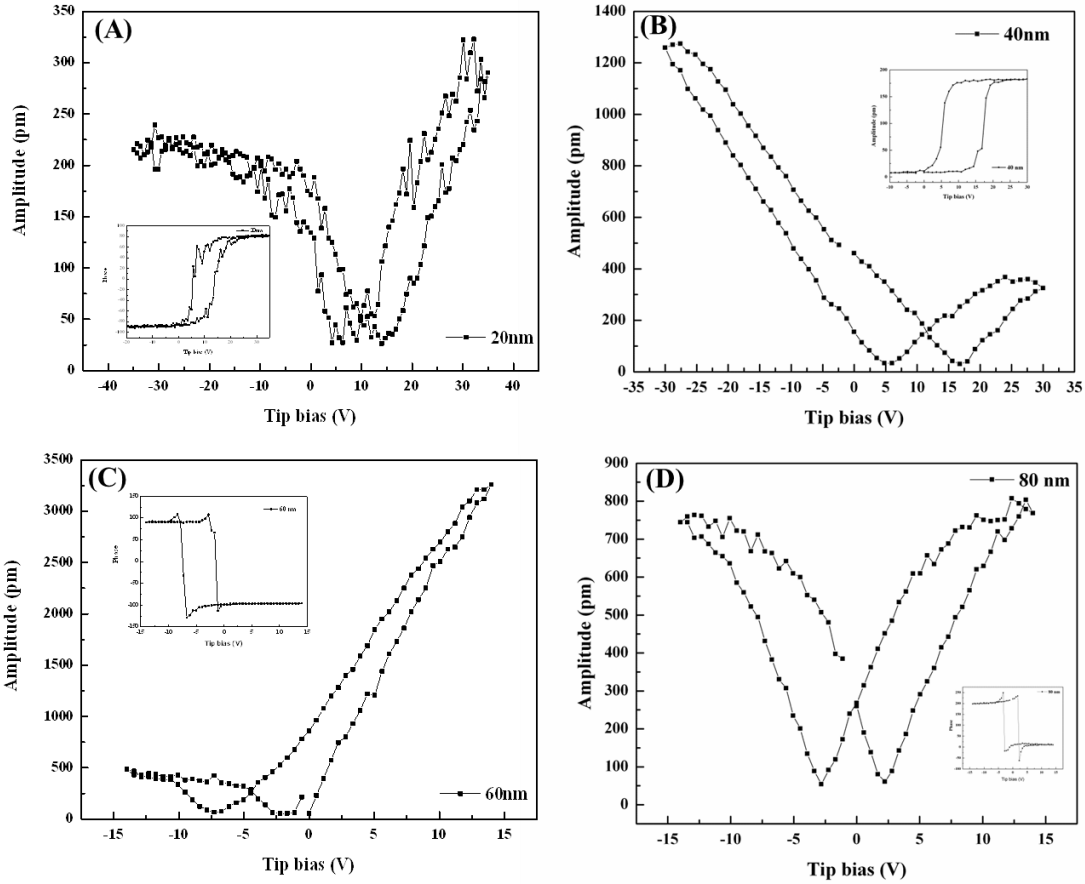


Figure S8 PFM switching spectroscopy shows amplitude and phase(inset) hyteresis loops for **(A)** 20 nm **(B)** 40 nm **(C)** 60 nm and **(D)** 80 nm thin films grown on NGO substrates

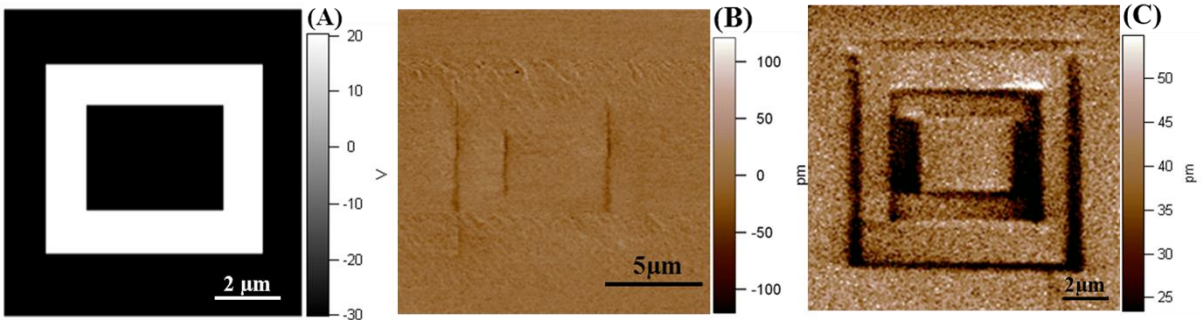


Figure S9 PFM **(A)** poling pattern with tip voltages ± 30V **(B)** amplitude image after poling of 20nm a-TiO_2 thin film on STO substrate **(C)** amplitude image after poling NGO substrate surface. There is no amplitude contrast in the images **(A)** and **(C)** showing the absence of poling due to electrostatic effects from the substrate.